

# DISTORTION IN SINGLE PHASE CURRENT CONTROLLED PV INVERTERS FOR GRID CONNECTION

R Sharma and T Ahfock  
Faculty of Engineering & Surveying  
University Of Southern Queensland  
Toowoomba 4350.

## Abstract

Unipolar switched single-phase inverters experience lower switching losses and cause less EMI when compared with bipolar switched inverters. However, these benefits come at the expense of increased distortion in the current waveform near the voltage zero-crossing. Moreover, it is demonstrated in this paper that switching delay causes generation of low frequency harmonics in the current waveform. In spite of that, unipolar switched inverters can be designed to operate within harmonic limits specified by the Australian Standard 4777.2.

## 1. INTRODUCTION

The conversion efficiency of single-phase, PWM, current controlled inverters can be improved by using unipolar switching [1]. Significant reduction in voltage transitions during switching is also an advantage from the point of view of EMI generation.

The advantages of current control such as active current wave shaping, inherent current limitation, automatic synchronisation with the utility grid and elimination of lower order harmonics has been realised [2]. For simplicity and excellent dynamic performance characteristics the current loop may be based on hysteretic control [3].

It could be postulated that a unipolar switched inverter with hysteretic current control will have all the advantages listed above. But such inverters also have inherent problems that may need attention. These include:

- (a) variation in the inverter switching frequency along the AC current waveform [4,5];
- (b) increased distortion near the voltage zero crossing [6]; and
- (c) generation of low frequency harmonics due to switching delay.

The last one of those problems is the focus of this paper. An analysis of hysteretic switching is carried out for both the unipolar switched inverter and the bipolar switched inverter. The objective of the analysis is to confirm that switching delay causes low frequency distortion in unipolar switched inverters with hysteretic current control.

The paper also explores the question of compliance to Australian Standard 4777.2.

## 2. INVERTER SYSTEMS

Figure 1 shows a simplified diagram of the inverter voltage control loop (VCL) and current control loop (CCL). The function of the VCL is to keep the DC voltage relatively constant. In doing so, balance between input DC power and output AC power is achieved. Increased insolation level will cause the bulk capacitor voltage  $v_c$  to tend to rise. This in turn causes the DC voltage error  $v_e$  and AC reference current  $i_{sref}$  to increase. The current controller provides switching signals for the inverter switches so that  $i_p$  closely follows  $i_{sref}$  causing the AC power to rise and match the increased DC power.

Current control may be based on unipolar switching or bipolar switching.

### 2.1 Unipolar Mode

Hysteretic control with a fixed tolerance band,  $I_{tol}$ , is used to force current  $i_p$  to track the reference sinusoidal current  $i_{sref}$ . The controller forces the bridge into one of four possible states depending on the need to make  $|i_p|$  rise or fall and on the polarity of  $v_s$ . Whenever  $|i_p|$  is falling and reaches the bottom current limit,  $|i_p| - 0.5I_{tol}$ ,  $|i_p|$  is made to rise by switching on  $T_{A+}$  and  $T_{B-}$  if  $v_s$  is positive or  $T_{B+}$  and  $T_{A-}$  if  $v_s$  is negative. Due to circuit component imperfections there is a time delay  $t_d$  between the instant  $|i_p|$  reaches the bottom current limit and the instant the inverter changes state (Figure 2). Whenever  $|i_p|$  reaches the top current limit,  $|i_p| + 0.5I_{tol}$ ,  $|i_p|$  is made to fall by turning off one of the previously conducting pair of transistors. Again

there is a time delay between the instant  $\left| \dot{i}_p \right|$  reaches the top limit and the instant the inverter changes state.

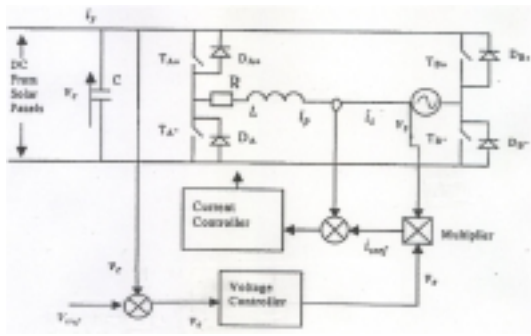


Figure 1: Single-phase grid connected PV inverter system.

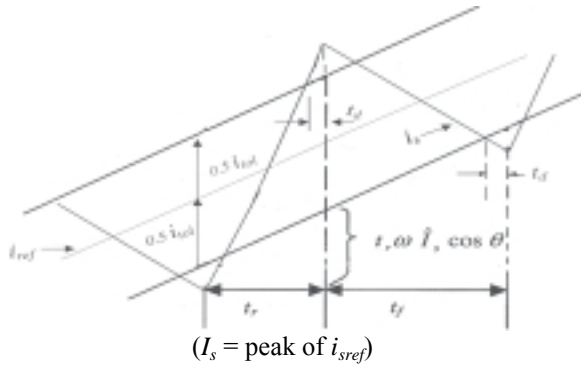


Figure 2: Hysteretic current control

### 2.2 Bipolar Mode

Figures 1 and 2 are applicable. If we ignore blanking times the inverter operates in one of two states. Transistors  $T_{A+}$  and  $T_{B-}$  are switched on when current  $i_s$  reaches the bottom limit of the tolerance band. Transistors  $T_{B+}$  and  $T_{A-}$  are switched on when current  $i_s$  reaches the top limit. There is a time delay between the instant when  $i_s$  reaches a tolerance band limit and the instant the inverter changes state.

### 3. Low Frequency Distortion

SIMULINK® models were used to simulate unipolar and bipolar switching. Figure 3 shows the unipolar switching model and a similar model was developed for bipolar switching. The inverter switches were assumed to be perfect. An RLC ripple filter was added to filter out switching frequency harmonics (figure 4). The following values were used:

$$V_s = 240 \text{ V}; I_{tol} = 0.2 \text{ A}; V_c = 400 \text{ V};$$

$$I_{ref} = 4.0 \text{ A and } 0.5 \text{ A}; t_d = 2 \mu\text{s and } 8 \mu\text{s};$$

$$C_f = 2 \mu\text{F}; L_1 = 8.0 \text{ mH}; L_2 = 2.0 \text{ mH}; R_c = 5 \Omega ;$$

The rationale behind the choice of component values for the filter components is given in reference 5. That filter has practically no effect on low frequency harmonics.

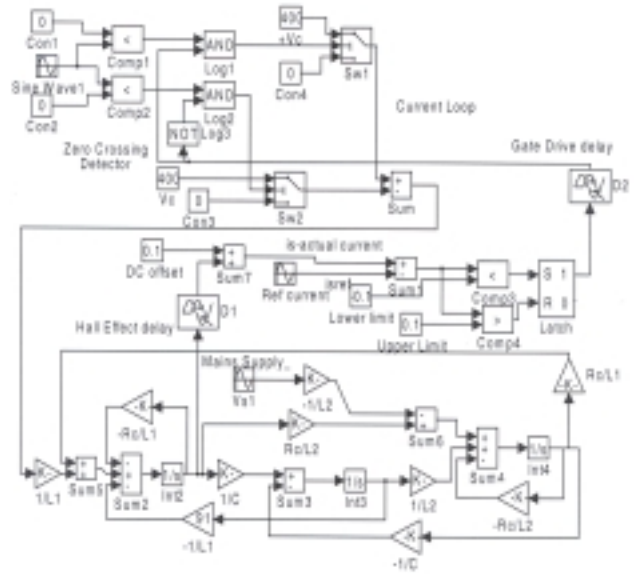


Figure 3 SIMULINK model of the current loop

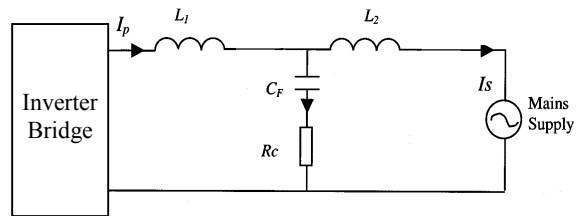
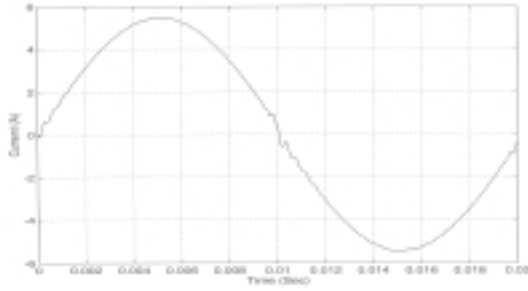


Figure 4: Ripple filter configuration

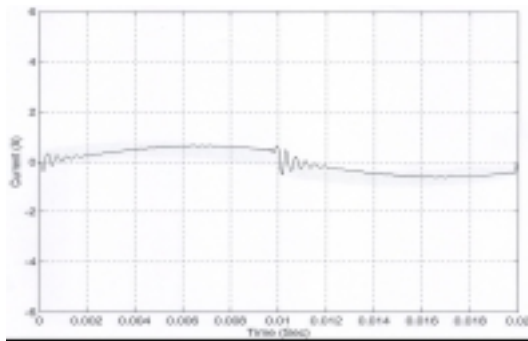
The time delay  $t_d$  represents a combination of component delays including current sensor, gate drive and main switching transistor. On grounds of power loss minimisation a Hall effect current sensor is preferred compared to a shunt resistor. However there is usually a need to keep cost down and this means that the quality of the selected Hall effect sensor will be such that it outputs a signal that is delayed. by, typically, a few microseconds compared with the actual current. The above values of  $t_d$  have been chosen to reflect this.

Simulation results are shown in figures 5 and 6. Harmonic analysis carried out on the current waveforms reveals significant levels of low frequency harmonics in the output of the unipolar switched inverter, whereas they are practically non-existent in

the case of the bipolar switched inverter (figures 7 and 8).

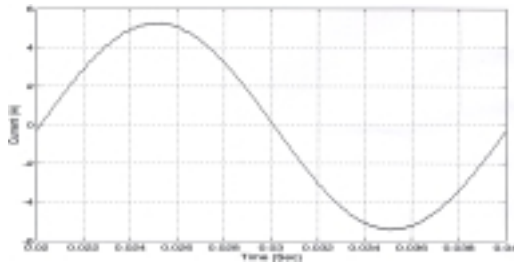


(a) Inverter supplying 4.0 A

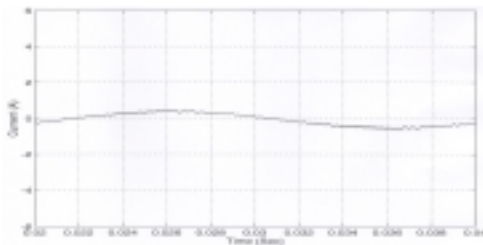


(b) Inverter supplying 0.5 A

Figure 5: Filtered output current from unipolar switched inverter

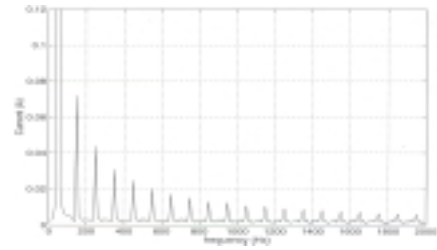


(a) Inverter supplying 4.0 A

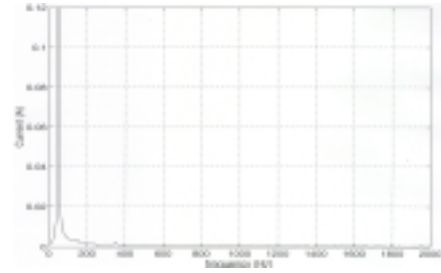


(b) Inverter supplying 0.5 A

Figure 6: Filtered output current from bipolar switched inverter



(a) Unipolar Inverter supplying 0.5 A ( $td = 8 \mu s$ )



(b) Bipolar Inverter supplying 0.5 A ( $td = 8 \mu s$ )

Figure 7: Low Frequency current harmonics

#### 4. Origin of Low Frequency Harmonics

Refer to figure 2. Reference current  $i_{sref}$ , the bottom limit of the tolerance band and the top limit of the band are all varying sinusoidally at power frequency. But over the relatively short duration of one inverter switching cycle, they can all be assumed to be straight lines. It is also assumed that  $i_s$  rises and falls linearly during a switching cycle. Based on those assumptions, expressions will be derived for  $i_{av}$  which represents current  $i_p$  averaged over one inverter switching cycle. Current  $i_{av}$ , although averaged, is a function of time and may be regarded as current  $i_p$  with all the switching frequency harmonics filtered by a ripple filter but with any low frequency harmonic remaining intact.

##### 4.1 Unipolar Switching

During the rise time of  $i_p$  we have:

$$L \frac{di}{dt} = V_c - \hat{V}_s \sin \theta \quad (1)$$

Therefore:

$$t_r = \left( L I_{tol} + t_d \frac{V_c}{V_c} \right) / \left( V_c - \hat{V}_s \sin \theta - L \omega \hat{I}_{sref} \cos \theta \right) \quad (2)$$

Similarly during the current fall-time we have:

$$L \frac{di}{dt} = -\hat{V}_s \sin \theta \quad (3)$$

$$t_f = \left( LI_{tol} + t_d V_c \right) / \left( \hat{V}_s \sin \theta + L\omega \hat{I}_{sref} \cos \theta \right) \quad (4)$$

The ripple free current  $i_{av}$  is given by:

$$i_{av}(\theta) = 1/(t_r + t_f) \{ [\hat{I}_{sref} \sin \theta - 0.5I_{tol} - (t_d \hat{V}_s \sin \theta)/L] t_r + (V_c - \hat{V}_s \sin \theta) t_r^2 / 2L - (\hat{V}_s \sin \theta) t_f^2 / 2L + [\hat{I}_{ref} \sin \theta + 0.5I_{tol} + t_d (V_c - \hat{V}_s \sin \theta)/L] t_f \} \quad (5)$$

The following can be deduced from equation 5:

- If switching delay is set to zero, not surprisingly, current  $i_{av}$  matches the reference current  $i_{ref}$  exactly.
- A non-zero switching delay results in  $i_{av}$  being higher than  $i_{ref}$  for half of the time and lower for the other half (figure 8) signifying the presence of low frequency distortion.
- Percentage distortion due to low frequency harmonics is much higher at lower output current (figure 8 (b)).

The fundamental reason for  $i_{av}$  being higher than  $i_{sref}$  at lower values of  $v_s$  is that  $i_p$  is driven by a higher voltage, which is  $V_c - |v_s|$ , when it is rising above the top tolerance limit compared to the voltage,  $|v_s|$ , that drives  $i_p$  when it is falling below the bottom limit. Similarly  $i_{av}$  is lower than  $i_{sref}$  at higher values of  $v_s$  because  $i_s$  is driven by a lower voltage, which is  $V_c - |v_s|$ , when it is rising above the upper tolerance limit and by a higher voltage,  $|v_s|$ , when it is falling below the bottom limit.

## 4.2 Bipolar Switching

During the rise time of  $i_p$  we have:

$$L \frac{di}{dt} = V_c - \hat{V}_s \sin \theta \quad (6)$$

Therefore:

$$t_r = \left( LI_{tol} + 2t_d V_c \right) / \left( V_c - \hat{V}_s \sin \theta - L\omega \hat{I}_{ref} \cos \theta \right) \quad (7)$$

Similarly during the current fall-time we have:

$$L \frac{di}{dt} = -V_c - \hat{V}_s \sin \theta \quad (8)$$

$$t_f = \left( LI_{tol} + 2t_d V_c \right) / \left( V_c + \hat{V}_s \sin \theta + L\omega \hat{I}_{ref} \cos \theta \right) \quad (9)$$

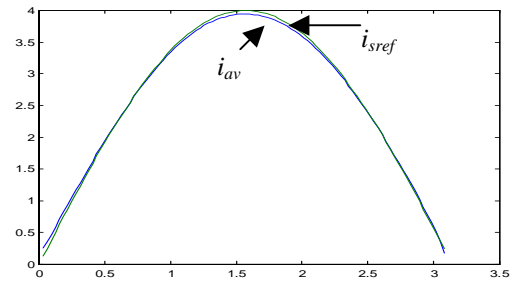
The ripple free current  $i_{av}$  is given by:

$$i_{av}(\theta) = 1/(t_r + t_f) \{ [\hat{I}_{ref} \sin \theta - 0.5I_{tol} - t_d (V_c + \hat{V}_s \sin \theta)/L] t_r + (V_c - \hat{V}_s \sin \theta) t_r^2 / 2L - (V_c + \hat{V}_s \sin \theta) t_f^2 / 2L + [\hat{I}_{ref} \sin \theta + 0.5I_{tol} + t_d (V_c - \hat{V}_s \sin \theta)/L] t_f \} \quad (10)$$

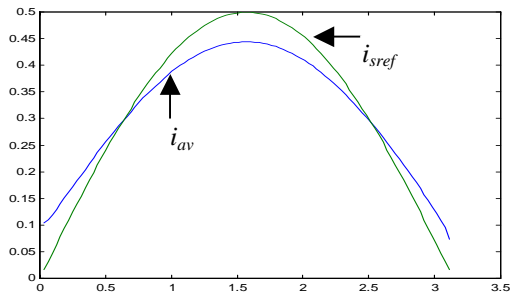
The following can be deduced from equation 10:

- As in the unipolar case, if switching delay is set to zero current  $i_{av}$  matches the reference current exactly.
- Current  $i_{av}$  is always lower than  $i_{sref}$  with the difference at a given time instant being proportional to the value of  $i_{sref}$  at that instant. This signifies that although  $i_{av}$  is lower than  $i_{sref}$ , there is no harmonic content in  $i_{av}$ .
- The percentage difference between current  $i_{av}$  and current  $i_s$  is higher at lower inverter output current (figure 9).

The fundamental reason for  $i_{av}$  being lower than  $i_{sref}$  is that  $i_p$  is driven by a lower voltage, which is  $V_c - |v_s|$ , when it is rising above the top tolerance limit and by a higher voltage, which is  $V_c + |v_s|$ , when it is falling below the bottom tolerance limit. The difference between those two voltages is equal to twice  $v_s$ , which is sinusoidal. This makes the difference between  $i_{av}$  and  $i_s$  sinusoidal implying that  $i_{av}$  is harmonic free.

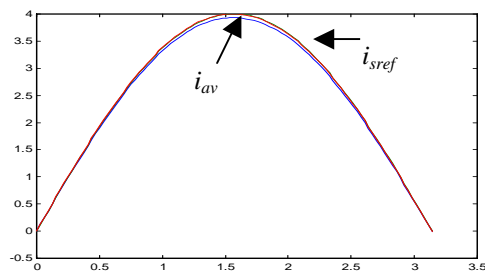


(a) Inverter supply 4.0 A

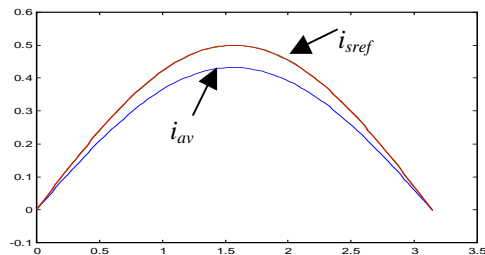


(b) Inverter supply 0.5 A

Figure 8: Unipolar Switched Inverter: Output Current with Switching Ripple Removed.



(a) Inverter supply 4.0 A



(b) Inverter supply 0.5 A

Figure 9: Bipolar Switched Inverter: Output Current with Switching Ripple Removed

## 5. Practical Implications

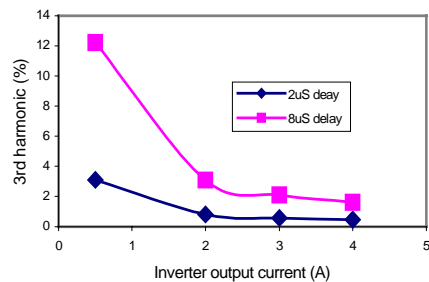


Figure 10: Unipolar: Effect of delay on 3<sup>rd</sup> harmonics

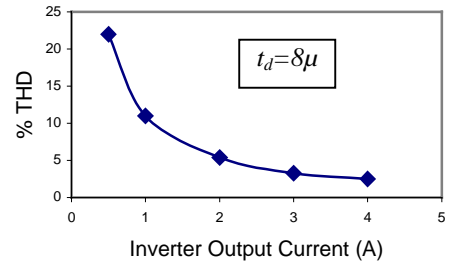


Figure 11: Unipolar: Total harmonics Distortion

An inverter selected for in grid-connected PV applications has to meet the requirements of a relevant standard that specifies distortion limits. In Australia this would be AS4777.2. The question is whether the levels of low frequency harmonics in the output of unipolar inverters fall within the limits specified by the standard. This question is best answered on a case by case basis. For the inverter considered in section 3 above, the third harmonic is the worst one and its levels are shown in figure 10. Total harmonic distortion is shown in figure 11. It has been assumed that non-zero switching delay is the only reason for the generation of low frequency harmonics. The inverter is designed for a rated output of 4 A, therefore it would satisfy the requirements of AS4777.2 even if switching delay is as high as 8  $\mu$ s. Individual levels for the second to the ninth harmonic should be limited to 4% whereas total harmonic distortion should be limited to 5% [7].

## 6. CONCLUSION

Switching delay causes low frequency distortion in grid-connected unipolar switched inverters using hysteretic current control. A simple switching model has been used to explain how low frequency harmonics are generated. It has been shown that the unipolar inverter can still be designed to meet the requirements of AS4777.2. In spite of that, methods to reduce the percentage THD at low lower levels are currently being investigated.

## 7. References

- [1]. Liaw C M, Chen T H, Wang T C, Cho G J, Lee C M and Wang C T, "Design and Implementation of a Single Phase Current-Forced Switching Mode Bilateral Converter", IEEE Proceedings PtB, No.3, pp 129-136, May 1991.
- [2]. Borle L, Dymond M S, Nayar C V, Philips S J, "Current Controlled Grid Connected Inverter", Proceedings of the Australian and New Zealand Solar

Energy Society Conference, pp 374-379, December 1993.

[3]. Harashima F, Inaba H, Kondo S, Takashima N, "Microprocessor-Controlled SIT Inverter for Solar Energy Systems", IEEE Transactions on Industrial Electronics", pp 50-55, Vol 34, No. 1, February 1987.

[4] Szepesi T, "Stabilising the Frequency of Hysteretic Current-Mode D.C./D.C. Converters", IEEE Transactions on Power Electronic, pp 302- 312, Vol 2, No. 4, October 1987.

[5] Sharma R, "Switching Frequency Filter Design For Utility Connected PV Inverters", Australasia Universities Power Engineering Conference Proceedings, September-October 2002.

[6]. Sharma R, "Analysis of PWM Transformerless Inverter for Utility Connected PV Applications", Australasia University Power Engineering Conference Proceedings, September 2001.

[7] Australian Standards AS4777.2, 2002, "Grid connection of energy systems via inverters", Part 2 : Inverter requirements.